



High-grade glioma imaging volumes and survival: a single-institution analysis of 101 patients after resection using intraoperative MRI

Nicholas T. Gamboa¹ · Brendan Crabb² · Jeffrey Curran Henson³ · Kyril L. Cole² · Bradley D. Weaver² · Michael Karsy¹ · Randy L. Jensen^{1,4}

Received: 25 August 2022 / Accepted: 5 October 2022 / Published online: 17 November 2022
© The Author(s), under exclusive licence to Springer Science+Business Media, LLC, part of Springer Nature 2022

Abstract

Purpose Intraoperative magnetic resonance imaging (iMRI) has been efficacious in maximizing resection of high-grade gliomas (HGGs). In this single-institution study of patients with HGGs who underwent resection using iMRI, the authors present a volumetric-based survival analysis to evaluate progression-free survival (PFS) and overall survival (OS), as well as the impact of additional resection on survival.

Methods This retrospective analysis included patients with HGGs who underwent resection using iMRI from 2011 to 2021. Volumetric analyses of T1-weighted contrast-enhancing (T1W-CE), T2-weighted (T2W), and T2W fluid-attenuated inversion recovery (FLAIR) MRI sequences were assessed at preoperative, intraoperative, immediate postoperative, and three-month postoperative timepoints. Statistical analyses were carried out using log-rank and multivariable Cox proportional hazard regression analyses.

Results A total of 101 patients (median age 57.0 years) were treated. In keeping with prior studies, statistically significant associations between greater EOR and longer PFS and OS were seen ($p=0.012$ and $p=0.006$, respectively). The results demonstrated significant associations between lower preoperative T2W, 3-month postoperative T2W, and 3-month postoperative FLAIR volumes with longer PFS and OS ($p=0.045$ and $p=0.026$, $p=0.031$ and $p=0.006$, $p=0.018$ and $p=0.004$, respectively), as well as associations between lower immediate postoperative T2W and immediate postoperative FLAIR volumes with longer OS ($p=0.002$ and $p=0.02$). There was no observed association in either PFS or OS for patients undergoing additional resection after initial iMRI scan ($p=0.387$ and $p=0.592$).

Conclusion This study of 101 patients with new or recurrent HGGs shows three-month postoperative T2W and FLAIR imaging volumes were significant prognosticators with respect to PFS and OS.

Keywords Extent of resection · Glioblastoma · High-grade glioma · Intraoperative MRI · Volumetric analysis · Survival · Tumor volumes

✉ Randy L. Jensen
neuropub@hsc.utah.edu

¹ Department of Neurosurgery, Clinical Neurosciences Center, University of Utah, 175 N. Medical Drive East, Salt Lake City, UT 84132, USA

² School of Medicine, University of Utah, Salt Lake City, UT, USA

³ College of Medicine, University of Arkansas for Medical Sciences, Little Rock, AR, USA

⁴ Departments of Oncological Sciences and Radiation Oncology, University of Utah, Salt Lake City, UT, USA

Introduction

Glioblastoma (GBM) is the most common malignant brain tumor in adults, comprising 15% of all intracranial tumors, 45–50% of all primary brain tumors, and 55–57% of all gliomas [1, 2]. This World Health Organization (WHO) grade IV astrocytic neoplasm is characterized by its aggressive and diffusely infiltrative nature, which portends its poor prognosis [3]. Despite genomic, technologic, therapeutic, and operative advancements in the treatment of GBM, it remains invariably fatal, with an average overall survival (OS) of 15–18 months and just 6.8% of patients surviving 5 years after diagnosis [1, 2, 4, 5]. The role of surgery in the treatment of GBM and other similar-behaving

IDH wild-type high-grade gliomas (HGGs) has been extensively studied and refined in recent decades, with particular attention towards so-called “cytoreductive surgery” or improved extent of resection (EOR) [6–9]. Numerous studies have demonstrated that greater EOR is independently associated with longer progression-free survival (PFS) and OS, symptom palliation, and improved quality of life in patients with both low- and high-grade gliomas [7, 10–16]. Although much attention has been paid to EOR as an independent prognosticator, several recent studies have argued that contrast-enhancing residual tumor volumes (CE-RTVs) are a more important predictor of survival after HGG resection—because EOR is significantly influenced by preoperative tumor volume [17–21]. Accordingly, several assistive technologies—including intraoperative magnetic resonance imaging (iMRI) and fluorescence-guided resection using 5-aminolevulinic acid—have been developed to safely improve EOR and decrease CE-RTV [22–28].

Since its introduction in the mid-1990s, iMRI has been demonstrated to maximize EOR and survival while reducing CE-RTV in patients with HGGs when compared with conventional stereotactic navigation alone [24, 26, 27, 29, 30]. Many of these studies have focused primarily on the relationship of survival parameters (i.e., PFS and OS) with EOR or immediate CE-RTV measurements [29, 31–33]. We present a single-institution analysis of patients with HGGs who were treated surgically over a 10-year period using iMRI. In this study, we compared pre-, intra-, immediate post-, and three-month postoperative T1-weighted (T1W) and T2-weighted (T2W) imaging volumes and their relationship with PFS and OS. Further, we examine those patients who underwent additional resection after initial iMRI scans, the likelihood of positive pathologic margins, and the relationship of additional resection with PFS and OS.

Methods

Patient population and study design

The study was a retrospective review of a prospectively maintained database of patients with HGG treated surgically using a 3.0T iMRI at the University of Utah and the 1.5T iMRI at the Huntsman Cancer Institute over a 10-year period from December 2011 to October 2021. The initial cohort consisted of 125 total patients with pathology-proven GBM (isocitrate dehydrogenase [IDH] wild-type or IDH mutated) or WHO grade III anaplastic astrocytoma (IDH wild-type only) who underwent resection using iMRI. Exclusion criteria included patients who did not have progression or survival data, *IDH1/2* or O⁶-methylguanine-DNA methyltransferase (*MGMT*) biomarker data, or those patients

whose tumors were determined to be *IDH1/2* mutant. Patients were also excluded if they lacked imaging data available at the time points of interest: preoperative MRI with and without gadolinium contrast, iMRI with and without gadolinium contrast, immediate postoperative MRI with and without gadolinium contrast, and three-month postoperative MRI with and without gadolinium contrast. For patients who underwent more than one iMRI scan, the last scan performed was used to obtain the volumetric data for analysis. A total of 24 patients were excluded from the analyses based on these exclusion criteria. The final patient cohort used in the analyses included 101 patients with new or recurrent IDH wild-type HGGs. Patient demographics, progression and survival data, pathological reports with tumor-specific markers, and imaging records were obtained. Although many other patients with HGG were treated surgically during the study’s 10-year duration, a large number were resected using conventional stereotactic navigation and/or 5-aminolevulinic acid fluorescence-guided resection, thus precluding them from the present study cohort.

Data collection

Minimum MRI sequences obtained included axial T1W non-contrast, axial T1W post-contrast, axial T2W, axial T2 fluid-attenuated inversion recovery (FLAIR), and axial diffusion-weighted imaging (DWI) with apparent diffusion coefficient sequences. Preoperative, intraoperative, immediate postoperative (within 24 h of surgery), and three-month postoperative scans were downloaded from the hospital picture archiving and communication system to an OsiriX DICOM viewer (Pixmeo SARL, Bernex, Switzerland). Radiological volume data from each time point of interest included T1W non-contrast hyperintense volumes, T1W contrast-enhancing (CE) tumor volumes, T2W hyperintense volumes, and FLAIR hyperintense volumes.

Clinical variables were collected in prospective fashion, and survival data were updated retrospectively. Clinical variables included age, sex, primary presenting sign/symptom, tumor location (lobe and laterality), date of surgery, date of progression, recurrence status, date of death, preoperative and 1-month postoperative Karnofsky Performance Scale (KPS) scores, whether patients underwent subsequent resection after the initial iMRI scan and whether these residual margins were positive on pathological analysis, and tumor-specific markers (i.e., *MGMT*, *TP53*, *PTEN*, *EGFR*, and *MIB-1*).

Imaging and volumetric analysis

Using the OsiriX DICOM viewer, three authors (N.T.G., J.C.H., and R.L.J.) measured the quantitative volumes by

using contours of axial T1W or T2W imaging. CE-RTVs were calculated by subtracting T1W non-contrast hyperintense volumes from T1W-CE volumes to subtract out postoperative blood products. Volumetric data for each patient was measured after surgery. The EOR was calculated using the following formula: [preoperative CE tumor volume – CE residual tumor volume / preoperative CE tumor volume] \times 100%. The initial iMRI scans were performed only after a gross total resection was achieved intraoperatively using both stereotactic neuronavigation and visual inspection with the microscope and with the attending surgeon's independent approval. To obtain a more granular understanding of tumor resection for each patient at different timepoints of their care, ratios were calculated for individual patients using postoperative/intraoperative and three-month postoperative/intraoperative T1W-CE, T2W, and FLAIR imaging volumes. The ratios were calculated to better understand relative disease burden for each patient at their various timepoints of treatment and to determine whether there was any relationship of these variables with PFS or OS.

Statistical analysis

All data analyses were performed using Jupyter Notebook software v4.4.0 in Python v3.6.8 programming language (Project Jupyter, open source; Python Software Foundation, Fredericksburg, VA) or using GraphPad Prism v9.4.1 (GraphPad Software, San Diego, CA). Descriptive statistics were obtained to define the patient cohort, including analyses of PFS and OS using T-test or Chi-square test. Patients were separated into groups that were above or equal to and below the median imaging volumes for all survival analyses. Using a log-rank test, imaging volume distributions were analyzed for their relationships with PFS and OS. A log-rank test was performed to examine EOR and its relationship with PFS and OS, as well as the relationship between further resection (after initial iMRI scan) and PFS and OS. Multivariable Cox proportional hazard regression analyses were also carried out for the imaging volumes from T1W-CE, T2W, and FLAIR sequences at the timepoints of interest to assess their relationship with PFS and OS. Lastly, we examined the relationships between PFS and OS and the following imaging volume ratios using log-rank tests: immediate postoperative/intraoperative volumes and three-month postoperative/intraoperative volumes for T1W-CE, T2W, and FLAIR sequences. A two-tailed $p < 0.05$ was deemed statistically significant in all analyses.

Results

Patient and tumor characteristics

Patient characteristics and survival data for the 101 patients with GBM (IDH wild-type only) or anaplastic astrocytoma (IDH wild-type only) surgically resected using iMRI are shown in Table 1. The median age was 57 years old (range 22.9–85.0 years); younger patients had significantly better PFS and OS ($p = 0.015$ and $p = 0.002$, respectively). Although preoperative KPS was not significantly associated with PFS, it was associated with OS ($p = 0.04$). Postoperative KPS was significantly associated with both PFS and OS ($p = 0.0015$ and $p = 0.0002$, respectively). The median PFS for the patient cohort was 7.8 months (range 0.13–101.2 months), and the median OS was 14.0 months (range 0.13–101.2 months) (Fig. 1a). The most common location of tumors was the temporal lobe (31/101; 30.7%), followed by the parietal lobe (28/101; 27.7%) and frontal lobe (27/101; 26.7%). The tumor location was significantly associated with PFS ($p < 0.001$). Tumors were roughly equal with respect to laterality (right: 52/101; left: 49/101).

Tumor and surgery characteristics are shown in Table 1. Of the 101-patient cohort, 42 patients (41.6%) were newly diagnosed, and 59 patients (58.4%) had recurrent disease and had undergone prior maximal safe resections. Recurrence was significantly associated with decreased PFS and OS ($p = 0.019$ and $p = 0.04$, respectively). Separate log-rank analyses were performed for newly diagnosed HGGs and recurrent HGGs and are included in Online Resource Table 1 and Online Resource Figs. 1 and 2. All patients were *IDH1/2*-wild type (101/101; 100%), and the majority of patients were *MGMT* unmethylated (67/101; 67.7%). *MGMT* promoter methylation was associated with longer PFS and OS ($p = 0.03$ and $p = 0.08$, respectively). Of patients with available data, 49/81 (60.5%) were *EGFR* non-amplified, 73/90 (81.1%) had a *TP53* mutation, and 48/71 (67.6%) carried a *PTEN* mutation. The mean MIB-1% was 40% (range 5.0–95.0%). *EGFR* amplification status, *TP53* mutation, *PTEN* mutation, and MIB-1% were not associated with PFS or OS. The median EOR was 93.6% (range 11.4–100%), with 52 patients (51.5%) undergoing further resection after the initial iMRI scan. Of those 52 patients, 46 (88.5%) had pathology-proven positive margins on subsequent resection. EOR was significantly associated with both PFS and OS, but further resection after initial iMRI was associated with neither.

Table 1 Baseline patient, tumor, and surgical characteristics in 101 patients with new or recurrent HGG who underwent surgical resection using iMRI

| Variables | Value | <i>p</i> -value | |
|---|------------------------|-----------------|-----------|
| | | PFS | OS |
| Patient characteristics | | | |
| Median age in years (range) | 57.0 (22.9–85.0) | 0.015* | 0.002** |
| Sex | | | |
| Male | 52 (51.5%) | 0.66 | 0.11 |
| Female | 49 (48.5%) | | |
| KPS | | | |
| Preoperative, median (range) | 78.0 (50–100) | 0.13 | 0.04* |
| 1-month postoperative, median (range) | 72.5 (0–100) | 0.0015** | 0.0002*** |
| Survival | | | |
| Median PFS in months (range) | 7.8 (0.13–101.2) | - | |
| Median OS in months (range) | 14.0 (0.13–101.2) | - | |
| Tumor type | | | |
| GBM (IDH wild-type) | 91 (91%) | - | |
| Anaplastic astrocytoma (IDH wild-type) | 10 (10%) | - | |
| Newly diagnosed HGG | 42 (41.6%) | | |
| Recurrent HGG | 59 (58.4%) | 0.019* | 0.04* |
| Tumor Location | | | |
| Frontal | 27 (26.7%) | 0.001** | 0.09 |
| Temporal | 31 (30.7%) | | |
| Insular | 3 (2.9%) | | |
| Parietal | 28 (27.7%) | | |
| Occipital | 10 (9.9%) | | |
| Cerebellar | 2 (1.9%) | | |
| Tumor Laterality | | 0.58 | 0.71 |
| Right | 52 (51.5%) | | |
| Left | 49 (48.5%) | | |
| Markers/Pathologic Characteristics | | | |
| <i>MGMT</i> unmethylated | 67 (67.7%) | 0.03* | 0.08 |
| <i>EGFR</i> non-amplified | 49/81 (60.5%) | 0.96 | 0.79 |
| <i>p53</i> mutation | 73/90 (81.1%) | 0.57 | 0.87 |
| <i>PTEN</i> mutation | 48/71 (67.6%) | 0.14 | 0.10 |
| MIB-1% (range) | 40% (5.0–95.0%) | 0.81 | 0.81 |
| Surgery Characteristics | | | |
| Extent of resection (range) | 93.6% (11.0–100.0%) | 0.012* | 0.006** |
| Further surgical resection (%) | 52 (51.5%) | 0.387 | 0.592 |
| Tumor present on additional resection (%) | 46 (88.5%) | - | |

p* < 0.05; *p* < 0.01; ****p* < 0.001

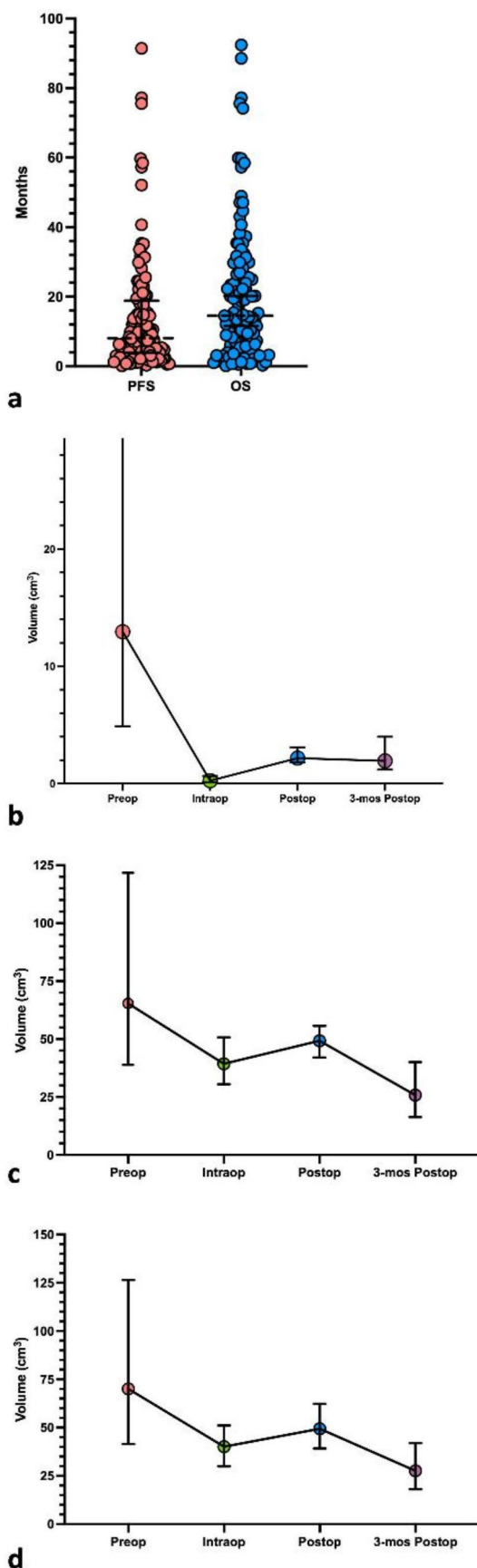
T1-weighted contrast-enhancing tumor volumes and survival

The median volumes and results of the log-rank analyses for the different imaging modalities at specific timepoints are summarized in Table 2. The temporal trend of T1W-CE tumor volumes for the patient cohort is depicted in Fig. 1b. It should be noted that a consistent trend of increase was seen in T1W-CE tumor volumes between intraoperative and immediate postoperative scans despite subtraction of blood products. Using a log-rank analysis of patients above and below the median volumes, There were no statistically significant associations observed for T1W-CE and PFS (Fig. 2a) or OS (Fig. 2b), but a consistent trend towards

longer PFS and OS is seen with below-median T1W-CE tumor volumes at all timepoints.

T2-weighted imaging volumes and survival

The temporal trend of T2W hyperintense volumes is depicted in Fig. 1c. In the log-rank analysis of patients above and below the median volumes at various timepoints, there was no association between intraoperative T2W volumes and PFS or OS (Fig. 2c,d), as well as no association found between immediate postoperative T2W volumes and PFS (Fig. 2c). However, there was a statistically significant association between smaller preoperative T2W volumes and longer PFS and OS (*p* = 0.045 and *p* = 0.026, respectively; Fig. 2c,d). A statistically significant association between lower immediate postoperative T2W volumes and better



◀ **Fig. 1** (a) Scatter plot showing median values and interquartile range for PFS and OS in the 101-patient cohort with new or recurrent IDH wild-type HGGs. Median values are represented by a dashed line. Error bars represent the interquartile range. Temporal trends of median T1W-CE (b), T2W (c), and FLAIR (d) imaging volumes (cm^3). T1W-CE, T2W, and FLAIR tumor volumes from preoperative (red), intraoperative (green), immediate postoperative (blue), and three-month postoperative (purple) MRI scans. The median value is represented by a colored circle. Error bars represent the interquartile range for each of the volumes

OS ($p=0.002$, Fig. 2d), as well as lower three-month postoperative T2W imaging volumes and longer PFS and OS ($p=0.031$ and $p=0.006$, respectively; Fig. 2c,d).

T2-FLAIR weighted imaging volumes and survival

The temporal trend of FLAIR hyperintense volumes is shown in Fig. 1d. On log-rank analysis of patients above and below the median volumes, there was no association between preoperative or intraoperative FLAIR volumes and PFS or OS (Fig. 2e,f) nor between immediate postoperative FLAIR volumes and PFS (Fig. 2e). A statistically significant association between smaller immediate postoperative FLAIR volumes and longer OS ($p=0.02$, Fig. 2f), as well as smaller three-month postoperative FLAIR volumes and better PFS and OS ($p=0.018$ and $p=0.004$, respectively; Fig. 2e,f).

Volumetric-based multivariable Cox proportional hazard regression analyses

A summary of the median volumes and results of the multivariable Cox proportional hazard regression analyses for the different imaging modalities at specific timepoints is summarized in Table 2. There was a statistically significant association between smaller intraoperative and three-month postoperative T1W-CE tumor volumes and PFS ($p=0.04$ and $p<0.005$, respectively). Only smaller three-month postoperative T1W-CE tumor volumes were significantly associated with better OS ($p<0.005$). There was no association seen for preoperative, intraoperative, or immediate postoperative T2W imaging volumes with PFS or OS. However, there was a statistically significant association between lower three-month postoperative T2W imaging volumes and PFS and OS ($p<0.005$ and $p=0.01$, respectively). Finally, no association was observed for preoperative, intraoperative, or immediate postoperative FLAIR imaging volumes with PFS or OS; however, a statistically significant association was seen between three-month postoperative FLAIR imaging volumes and PFS and OS ($p<0.005$ and $p=0.04$, respectively).

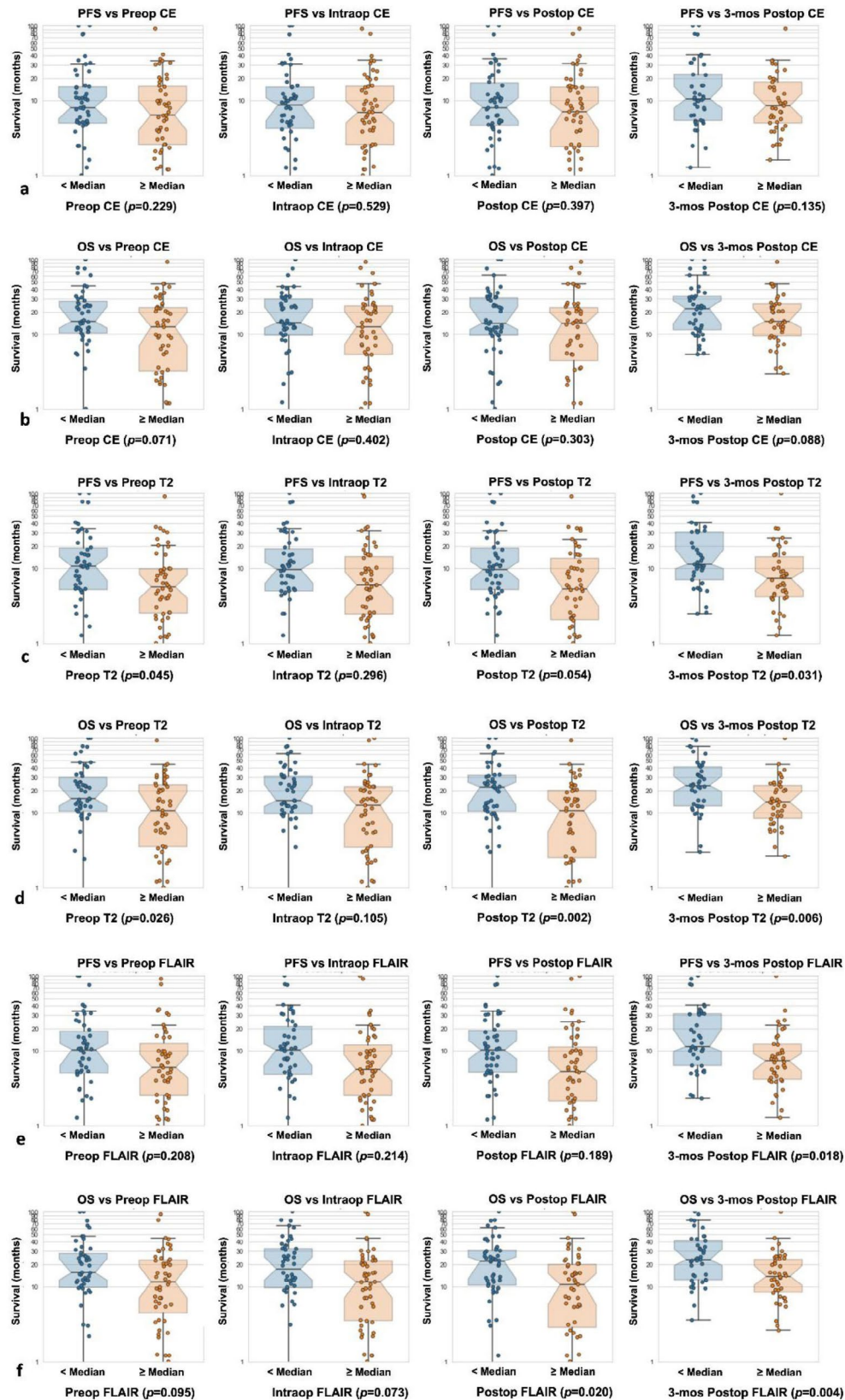


Fig. 2 Relationship of T1W-CE (a, b), T2W (c, d), and FLAIR (e, f), imaging volumes on PFS and OS. Log-rank analyses of preoperative, intraoperative, immediate postoperative, and three-month

postoperative imaging volumes—separated above and below the median—and their relationship with PFS and OS

Table 2 Imaging volumes and their relationships with PFS and OS at the timepoints of interest

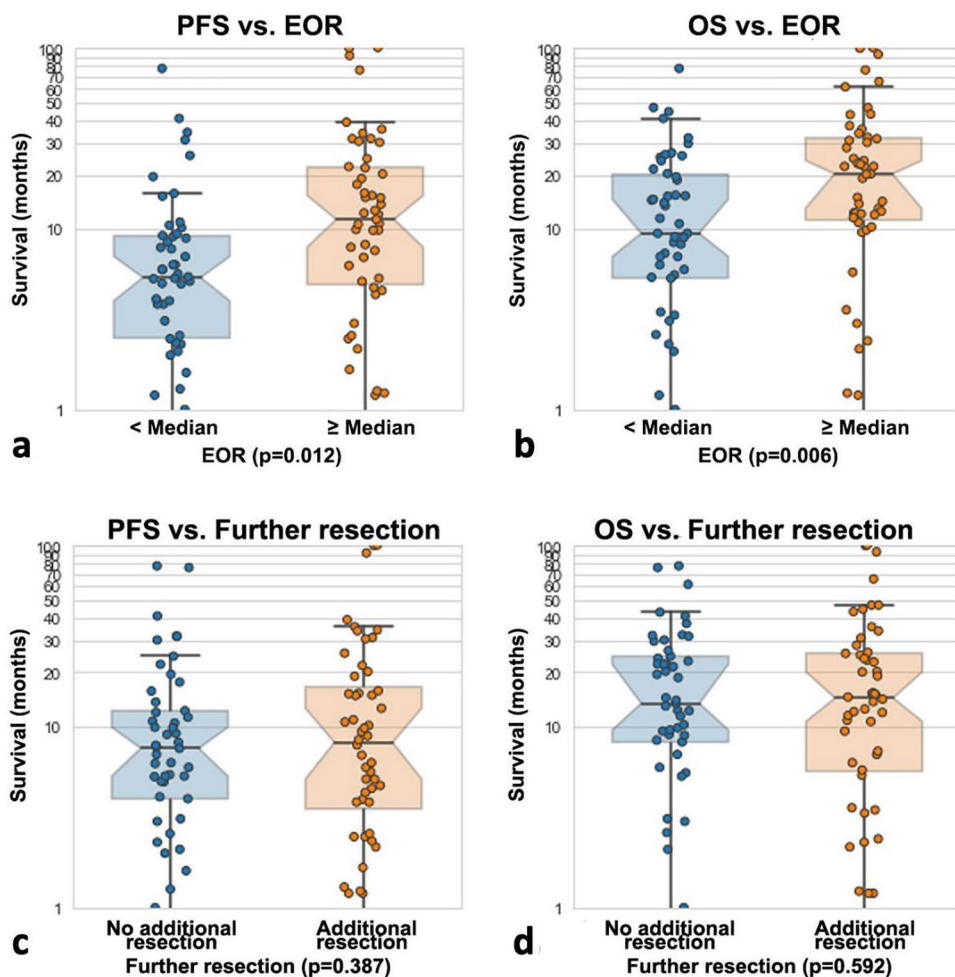
| Imaging Sequence | Timepoint | Median volume in cm ³ (range) | Log-rank <i>p</i> -values | | Multivariable Cox regression <i>p</i> -values | |
|-----------------------|------------------|--|---------------------------|---------|---|----------|
| | | | PFS | OS | PFS | OS |
| T1W-CE tumor volumes | Preop | 15.2 (0–83.8) | 0.229 | 0.07 | 0.35 | 0.87 |
| | Intraop | 0.62 (0–17.1) | 0.529 | 0.402 | 0.04* | 0.52 |
| | Immediate postop | 2.54 (0.0–21.1) | 0.397 | 0.303 | 0.33 | 0.22 |
| | 3-months postop | 1.7 (0.0–150.0) | 0.135 | 0.088 | <0.005** | <0.005** |
| T2W imaging volumes | Preop | 66.4 (2.2–310.1) | 0.045* | 0.026* | 0.19 | 0.86 |
| | Intraop | 38.6 (0.1–324.8) | 0.296 | 0.105 | 0.67 | 0.99 |
| | Immediate postop | 49.3 (0.34–331.2) | 0.054 | 0.002** | 0.06 | 0.81 |
| | 3-months postop | 23 (0.91–234.5) | 0.031* | 0.006** | <0.005** | 0.01* |
| FLAIR imaging volumes | Preop | 70.0 (0.31–305.2) | 0.208 | 0.095 | 0.19 | 0.65 |
| | Intraop | 41.4 (0.28–294.2) | 0.214 | 0.073 | 0.79 | 0.58 |
| | Immediate postop | 57.2 (1.1–327.0) | 0.189 | 0.02* | 0.05 | 0.48 |
| | 3-months postop | 28.7 (0.56–250.0) | 0.018* | 0.004** | <0.005** | 0.04* |

The median volumes and ranges for the three MRI sequences at the specific timepoints are also shown

p* < 0.05, *p* < 0.01

PFS, progression-free survival; OS, overall survival; T1W-CE, T1-weighted contrast-enhanced; T2W, T2-weighted; FLAIR, fluid-attenuated inversion recovery

Fig. 3 Relationship of EOR (a, b) and additional resection (c, d) on PFS and OS. Log-rank analysis of EOR separated above and below the median value and its relationship with PFS (a) and OS (b). Log-rank analysis of no additional resection versus additional resection and its relationship with PFS (c) and OS (d)



Extent of resection and survival

The median calculated EOR was 93.6% (range 11–100%). By log-rank analysis of EOR, patients were dichotomized above and below the median value. Statistically significant associations between greater EOR and both PFS and OS were seen (Fig. 3a,b).

Further resection, margin positivity, and survival

Fifty-two of 101 patients (51.5%) underwent additional resection after the initial iMRI scan. Tumor margins sent for final pathological analysis were positive for HGG in 46 patients (88.5%). In a log-rank analysis of patients who did or did not have additional resection, there was no observed improvement in either PFS ($p=0.387$) or OS ($p=0.592$) for patients undergoing additional resection after the initial iMRI scan (Fig. 3c,d).

Imaging sequence ratios and survival

Volumetric imaging ratios were calculated using the T1W-CE, T2W, and FLAIR sequence imaging volumes for each patient. There was no observed association with PFS or OS for any of the imaging volume ratios at any timepoint.

Discussion

In our single-center cohort of 101 patients with HGG, we evaluated the relationship of imaging volumes on different pre- and postoperative sequences with PFS and OS, along with the effect of additional resection after initial iMRI on survival. Our median EOR and OS were 93.6% and 14.0 months in this patient group, respectively. We identified that EOR and 3-month imaging volumes (i.e., T1W-CE, T2W, FLAIR) had the greatest association with OS. We also showed that additional surgical resection in 51.5% of cases after iMRI resulted in positive specimen in 88.5% of cases but did not improve survival in this patient group.

T1W imaging volumes

Numerous prior studies have shown that greater EOR and decreased CE-RTV (i.e., decreased intraoperative and postoperative T1W-CE tumor volumes) are both independently associated with longer PFS and OS [7, 10, 14–19, 21]. In our log-rank analysis of T1W-CE tumor volumes, there did not appear to be any association with PFS or OS; however, there was a consistent trend at all timepoints for longer PFS and OS with below-the-median T1W-CE tumor volumes. Although this was not entirely an expected result, we

attribute the lack of statistical significance primarily to the median EOR of 93.6% for this cohort. Our T1W-CE-based EOR calculations and log-rank analysis did show a statistically significant impact on both PFS ($p=0.012$) and OS ($p=0.006$).

T2W and FLAIR imaging volumes

Although much research has focused on T1W-CE tumor volumes and survival in patients with HGGs, a number of more recent studies have also demonstrated the prognostic importance of T2W and FLAIR imaging volumes [34, 35]. In the 1980s, Hochberg and Pruitt [36] first demonstrated via post-mortem examinations that 80% of HGGs recurred within 2 cm of the resection margin—where infiltrating tumor cells are highest in concentration. Accordingly, resection of hyperintense T2W/FLAIR tumor margins has been an area of significant interest. In 2016, Li et al. [12] examined 876 patients with GBM who underwent complete resection and found through multivariate analysis that those patients with >50% non-enhancing hyperintense FLAIR volume resection had significant improvement in OS. Grossman et al. [37] examined 103 patients with HGGs undergoing resection and found no significant association between immediate postoperative FLAIR volumes and OS. However, their study did show a statistically significant OS benefit when three-month postoperative FLAIR imaging volumes were below 19.3 cm³ [37].

In our log-rank analyses, lower immediate postoperative T2W and FLAIR imaging volumes were significantly associated with longer OS ($p=0.002$, $p=0.02$, respectively) but not PFS ($p=0.054$, $p=0.189$, respectively). However, on multivariate analyses there was no statistically significant association between PFS or OS and immediate postoperative T2W ($p=0.06$, $p=0.81$, respectively) or immediate postoperative FLAIR volumes ($p=0.05$, $p=0.48$, respectively). Similar to our T1W-CE volumetric analyses, we did see a consistent survival benefit for smaller T2W and FLAIR imaging volumes, likely suggesting our study was inadequately powered to detect a small but appreciable survival effect.

Our data showed a significant association between decreased volumes on three-month postoperative T2W and FLAIR and longer PFS ($p<0.005$, $p<0.005$) and OS ($p=0.01$, $p=0.04$). Collectively, we believe these data strongly support the prognostic value of T2W and FLAIR imaging volumes at three months postoperatively—with patients having significantly longer PFS and OS when three-month T2W volume is <23.0 cm³ and three-month FLAIR volume is <28.7 cm³.

iMRI utility

Lastly, we examined the effect of additional resection after initial iMRI scan on survival. Half of our patients underwent additional resection after iMRI use, with 88.5% of specimens containing tumor; however, there was no association of PFS or OS with undergoing additional surgical resection. This suggests that additional surgical resection after initial iMRI scan does not significantly improve nor worsen PFS or OS in patients with HGGs. This finding has been reported by other studies and meta-analyses evaluating iMRI use in HGGs [26, 32]. Likely, these results are not able to adjust for all the other heterogenous patient variables (e.g., age, tumor mutation, tumor location, EOR, complications, or postoperative treatment).

Limitations

This study represents a single-center series of patients with pathologically confirmed HGGs who underwent resection using iMRI. The limitations of this study include the likely skewed EOR distribution of patients in our cohort, with a median EOR of 93.6%, which makes our 101-patient cohort likely underpowered with respect to assessing T1W imaging-based survival associations. Additionally, most patients included in our cohort had recurrent disease (59/101; 58.4%), which likely confounded the overall PFS and OS of the cohort, as demonstrated in Online Resource Table 1 and Supplemental Figs. 1 and 2.

Conclusions

Our study of 101 patients with new or recurrent HGGs shows that three-month postoperative T2W and FLAIR imaging volumes may serve as significant prognosticators with respect to PFS and OS. In addition, our study did not demonstrate any improvement of PFS or OS for patients undergoing further resection after the initial iMRI scan.

Supplementary information The online version contains supplementary material available at <https://doi.org/10.1007/s11060-022-04159-5>.

Acknowledgements The authors thank Kristin Kraus, M.Sc., for her assistance with preparation of this publication.

Author contributions All authors contributed to the study conception and design. Acquisition of data was performed by Nicholas Gamboa, J. Curran Henson, and Randy Jensen. Drafting of article was by Nicholas Gamboa, Brendan Crabb, Kyril Cole, Bradley Weaver, Michael Karsy, and Randy Jensen. All authors contributed to statistical analysis and interpretation of all data. All authors reviewed the submitted final version of the manuscript.

Funding The authors declare that no funds, grants, or other support were received during the preparation of this manuscript.

Data availability The datasets generated during and/or analyzed during the current study can be made available in anonymized form from the corresponding author on reasonable request.

Statements and declarations

Competing interests Dr. Jensen is a consultant for Medtronic. The other authors have no relevant financial or non-financial interests to disclose.

Ethics approval This study was approved by the institutional review board at the University of Utah and Huntsman Cancer Institute in Salt Lake City, Utah (Protocol #0066337).

Consent to participate The need for informed consent was waived by the institutional review board.

Consent to publish The need for consent did not apply to this paper.

References

- Ostrom QT, Cioffi G, Gittleman H, Patil N, Waite K, Kruchko C, Barnholtz-Sloan JS (2019) CBTRUS Statistical Report: Primary Brain and Other Central Nervous System Tumors Diagnosed in the United States in 2012–2016. *Neuro Oncol* 21:v1–v100. <https://doi.org/10.1093/neuonc/noz150>
- Ostrom QT, Patil N, Cioffi G, Waite K, Kruchko C, Barnholtz-Sloan JS (2020) CBTRUS Statistical Report: Primary Brain and Other Central Nervous System Tumors Diagnosed in the United States in 2013–2017. *Neuro Oncol* 22:iv1–iv96. <https://doi.org/10.1093/neuonc/noaa200>
- Louis DN, Perry A, Wesseling P, Brat DJ, Cree IA, Figarella-Branger D, Hawkins C, Ng HK, Pfister SM, Reifenberger G, Soffietti R, von Deimling A, Ellison DW (2021) The 2021 WHO Classification of Tumors of the Central Nervous System: a summary. *Neurooncology* 23:1231–1251. <https://doi.org/10.1093/neuonc/noab106>
- Melin BS, Barnholtz-Sloan JS, Wensch MR, Johansen C, Il'yasova D, Kinnersley B, Ostrom QT, Labreche K, Chen Y, Armstrong G, Liu Y, Eckel-Passow JE, Decker PA, Labussière M, Idhah A, Hoang-Xuan K, Di Stefano AL, Mokhtari K, Delattre JY, Broderick P, Galan P, Gousias K, Schramm J, Schoemaker MJ, Fleming SJ, Herms S, Heilmann S, Nöthen MM, Wichmann HE, Schreiber S, Swerdlow A, Lathrop M, Simon M, Sanson M, Andersson U, Rajaraman P, Chanock S, Linet M, Wang Z, Yeager M, Wiencke JK, Hansen H, McCoy L, Rice T, Kosel ML, Sciotte H, Amos CI, Bernstein JL, Davis F, Lachance D, Lau C, Merrell RT, Schildkraut J, Ali-Osman F, Sadetzki S, Scheurer M, Shete S, Lai RK, Claus EB, Olson SH, Jenkins RB, Houlston RS, Bondy ML (2017) Genome-wide association study of glioma subtypes identifies specific differences in genetic susceptibility to glioblastoma and non-glioblastoma tumors. *Nat Genet* 49:789–794. <https://doi.org/10.1038/ng.3823>
- Rajaraman P, Melin BS, Wang Z, McKean-Cowdin R, Michaud DS, Wang SS, Bondy M, Houlston R, Jenkins RB, Wensch M, Yeager M, Ahlbom A, Albanes D, Andersson U, Freeman LE, Buring JE, Butler MA, Braganza M, Carreon T, Feychting M, Fleming SJ, Gapstur SM, Gaziano JM, Giles GG, Hallmans G, Henriksson R, Hoffman-Bolton J, Inskip PD, Johansen C,

- Kitahara CM, Lathrop M, Liu C, Le Marchand L, Linet MS, Lonn S, Peters U, Purdue MP, Rothman N, Ruder AM, Sanson M, Sesso HD, Severi G, Shu XO, Simon M, Stampfer M, Stevens VL, Visvanathan K, White E, Wolk A, Zeleniuch-Jacquotte A, Zheng W, Decker P, Enciso-Mora V, Fridley B, Gao YT, Kosel M, Lachance DH, Lau C, Rice T, Swerdlow A, Wiemels JL, Wiencke JK, Shete S, Xiang YB, Xiao Y, Hoover RN, Fraumeni JF Jr, Chatterjee N, Hartge P, Chanock SJ (2012) Genome-wide association study of glioma and meta-analysis. *Hum Genet* 131:1877–1888. <https://doi.org/10.1007/s00439-012-1212-0>
6. Stummer W, van den Bent MJ, Westphal M (2011) Cytoreductive surgery of glioblastoma as the key to successful adjuvant therapies: new arguments in an old discussion. *Acta Neurochir (Wien)* 153:1211–1218. <https://doi.org/10.1007/s00701-011-1001-x>
 7. Sanai N, Polley MY, McDermott MW, Parsa AT, Berger MS (2011) An extent of resection threshold for newly diagnosed glioblastomas. *J Neurosurg* 115:3–8. <https://doi.org/10.3171/2011.2.jns10998>
 8. Domino JS, Ormond DR, Germano IM, Sami M, Ryken TC, Olson JJ (2020) Cytoreductive surgery in the management of newly diagnosed glioblastoma in adults: a systematic review and evidence-based clinical practice guideline update. *J Neurooncol* 150:121–142. <https://doi.org/10.1007/s11060-020-03606-5>
 9. Noorbakhsh A, Tang JA, Marcus LP, McCutcheon B, Gonda DD, Schallhorn CS, Talamini MA, Chang DC, Carter BS, Chen CC (2014) Gross-total resection outcomes in an elderly population with glioblastoma: a SEER-based analysis. *J Neurosurg* 120:31–39. <https://doi.org/10.3171/2013.9.Jns13877>
 10. Brown TJ, Brennan MC, Li M, Church EW, Brandmeir NJ, Rakszawski KL, Patel AS, Rizk EB, Suki D, Sawaya R, Glantz M (2016) Association of the extent of resection with survival in glioblastoma: A systematic review and meta-analysis. *JAMA Oncol* 2:1460–1469. <https://doi.org/10.1001/jamaoncol.2016.1373>
 11. Beiko J, Suki D, Hess KR, Fox BD, Cheung V, Cabral M, Shonka N, Gilbert MR, Sawaya R, Prabhu SS, Weinberg J, Lang FF, Aldape KD, Sulman EP, Rao G, McCutcheon IE, Cahill DP (2014) IDH1 mutant malignant astrocytomas are more amenable to surgical resection and have a survival benefit associated with maximal surgical resection. *Neurooncology* 16:81–91. <https://doi.org/10.1093/neuonc/not159>
 12. Li YM, Suki D, Hess K, Sawaya R (2016) The influence of maximum safe resection of glioblastoma on survival in 1229 patients: Can we do better than gross-total resection? *J Neurosurg* 124:977–988. <https://doi.org/10.3171/2015.5.Jns142087>
 13. Marko NF, Weil RJ, Schroeder JL, Lang FF, Suki D, Sawaya RE (2014) Extent of resection of glioblastoma revisited: personalized survival modeling facilitates more accurate survival prediction and supports a maximum-safe-resection approach to surgery. *J Clin Oncol* 32:774–782. <https://doi.org/10.1200/jco.2013.51.8886>
 14. Orringer D, Lau D, Khatri S, Zamora-Berridi GJ, Zhang K, Wu C, Chaudhary N, Sagher O (2012) Extent of resection in patients with glioblastoma: limiting factors, perception of resectability, and effect on survival. *J Neurosurg* 117:851–859. <https://doi.org/10.3171/2012.8.Jns12234>
 15. Wang L, Liang B, Li YI, Liu X, Huang J, Li YM (2019) What is the advance of extent of resection in glioblastoma surgical treatment—a systematic review. *Chin Neurosurg J* 5:2. <https://doi.org/10.1186/s41016-018-0150-7>
 16. Molinaro AM, Hervey-Jumper S, Morshed RA, Young J, Han SJ, Chunduru P, Zhang Y, Phillips JJ, Shai A, Lafontaine M, Crane J, Chandra A, Flanigan P, Jahangiri A, Cioffi G, Ostrom Q, Anderson JE, Badve C, Barnholtz-Sloan J, Sloan AE, Erickson BJ, Decker PA, Kosel ML, LaChance D, Eckel-Passow J, Jenkins R, Villanueva-Meyer J, Rice T, Wrensch M, Wiencke JK, Oberheim Bush NA, Taylor J, Butowski N, Prados M, Clarke J, Chang S, Chang E, Aghi M, Theodosopoulos P, McDermott M, Berger MS (2020) Association of maximal extent of resection of contrast-enhanced and non-contrast-enhanced tumor with survival within molecular subgroups of patients with newly diagnosed glioblastoma. *JAMA Oncol* 6:495–503. <https://doi.org/10.1001/jamaoncol.2019.6143>
 17. Chaichana KL, Jusue-Torres I, Navarro-Ramirez R, Raza SM, Pascual-Gallego M, Ibrahim A, Hernandez-Hermann M, Gomez L, Ye X, Weingart JD, Olivi A, Blakeley J, Gallia GL, Lim M, Brem H, Quinones-Hinojosa A (2014) Establishing percent resection and residual volume thresholds affecting survival and recurrence for patients with newly diagnosed intracranial glioblastoma. *Neuro Oncol* 16:113–122. <https://doi.org/10.1093/neuonc/not137>
 18. Grabowski MM, Recinos PF, Nowacki AS, Schroeder JL, Angelov L, Barnett GH, Vogelbaum MA (2014) Residual tumor volume versus extent of resection: predictors of survival after surgery for glioblastoma. *J Neurosurg* 121:1115–1123. <https://doi.org/10.3171/2014.7.JNS132449>
 19. Ellingson BM, Abrey LE, Nelson SJ, Kaufmann TJ, Garcia J, Chinot O, Saran F, Nishikawa R, Henriksson R, Mason WP, Wick W, Butowski N, Ligon KL, Gerstner ER, Colman H, de Groot J, Chang S, Mellinghoff I, Young RJ, Alexander BM, Colen R, Taylor JW, Arrillaga-Romany I, Mehta A, Huang RY, Pope WB, Reardon D, Batchelor T, Prados M, Galanis E, Wen PY, Cloughesy TF (2018) Validation of postoperative residual contrast-enhancing tumor volume as an independent prognostic factor for overall survival in newly diagnosed glioblastoma. *Neuro Oncol* 20:1240–1250. <https://doi.org/10.1093/neuonc/ny053>
 20. Xing Y, Wang X (2018) Which parameter is more important for the prognosis of new-onset adult glioblastoma: residual tumor volume or extent of resection? *World Neurosurg* 116:e444–e451. <https://doi.org/10.1016/j.wneu.2018.05.003>
 21. Awad AW, Karsy M, Sanai N, Spetzler R, Zhang Y, Xu Y, Mahan MA (2017) Impact of removed tumor volume and location on patient outcome in glioblastoma. *J Neurooncol* 135:161–171. <https://doi.org/10.1007/s11060-017-2562-1>
 22. Gandhi S, Tayebi Meybodi A, Belykh E, Cavallo C, Zhao X, Syed MP, Borba Moreira L, Lawton MT, Nakaji P, Preul MC (2019) Survival outcomes among patients with high-grade glioma treated with 5-aminolevulinic acid-guided surgery: A systematic review and meta-analysis. *Front Oncol* 9:620. <https://doi.org/10.3389/fonc.2019.00620>
 23. Shah AS, Sylvester PT, Yahanda AT, Vellimana AK, Dunn GP, Evans J, Rich KM, Dowling JL, Leuthardt EC, Dacey RG, Kim AH, Grubb RL, Zipfel GJ, Oswood M, Jensen RL, Sutherland GR, Cahill DP, Abram SR, Honeycutt J, Shah M, Tao Y, Chicoine MR (2020) Intraoperative MRI for newly diagnosed supratentorial glioblastoma: a multicenter-registry comparative study to conventional surgery. *J Neurosurg* 1–10. <https://doi.org/10.3171/2020.6.Jns19287>
 24. Senft C, Bink A, Franz K, Vatter H, Gasser T, Seifert V (2011) Intraoperative MRI guidance and extent of resection in glioma surgery: a randomised, controlled trial. *Lancet Oncol* 12:997–1003. [https://doi.org/10.1016/s1470-2045\(11\)70196-6](https://doi.org/10.1016/s1470-2045(11)70196-6)
 25. Özduman K, Yıldız E, Dinçer A, Sav A, Pamir MN (2014) Using intraoperative dynamic contrast-enhanced T1-weighted MRI to identify residual tumor in glioblastoma surgery. *J Neurosurg* 120:60–66. <https://doi.org/10.3171/2013.9.Jns121924>
 26. Kubben PL, ter Meulen KJ, Schijns OE, Laak-Poort MP, van Overbeeke JJ, van Santbrink H (2011) Intraoperative MRI-guided resection of glioblastoma multiforme: a systematic review. *Lancet Oncol* 12: 1062–1070. [https://doi.org/10.1016/s1470-2045\(11\)70130-9](https://doi.org/10.1016/s1470-2045(11)70130-9)
 27. Golub D, Hyde J, Dogra S, Nicholson J, Kirkwood KA, Gohel P, Loftus S, Schwartz TH (2020) Intraoperative MRI versus 5-ALA in high-grade glioma resection: a network meta-analysis. *J Neurosurg* 1–15. <https://doi.org/10.3171/2019.12.Jns191203>

28. Eyüpoglu IY, Hore N, Savaskan NE, Grummich P, Roessler K, Buchfelder M, Ganslandt O (2012) Improving the extent of malignant glioma resection by dual intraoperative visualization approach. *PLoS ONE* 7:e44885. <https://doi.org/10.1371/journal.pone.0044885>
29. Napolitano M, Vaz G, Lawson TM, Docquier MA, van Maanen A, Duprez T, Raftopoulos C (2014) Glioblastoma surgery with and without intraoperative MRI at 3.0T. *Neurochirurgie* 60:143–150. <https://doi.org/10.1016/j.neuchi.2014.03.010>
30. Kuhnt D, Becker A, Ganslandt O, Bauer M, Buchfelder M, Nimsky C (2011) Correlation of the extent of tumor volume resection and patient survival in surgery of glioblastoma multiforme with high-field intraoperative MRI guidance. *Neuro Oncol* 13:1339–1348. <https://doi.org/10.1093/neuonc/nor133>
31. Zhang J, Chen X, Zhao Y, Wang F, Li F, Xu B (2015) Impact of intraoperative magnetic resonance imaging and functional neuronavigation on surgical outcome in patients with gliomas involving language areas. *Neurosurg Rev* 38:319–330. <https://doi.org/10.1007/s10143-014-0585-z>
32. Roder C, Bisdas S, Ebner FH, Honegger J, Naegele T, Ernemann U, Tatagiba M (2014) Maximizing the extent of resection and survival benefit of patients in glioblastoma surgery: high-field iMRI versus conventional and 5-ALA-assisted surgery. *Eur J Surg Oncol* 40:297–304. <https://doi.org/10.1016/j.ejso.2013.11.022>
33. Tsugu A, Ishizaka H, Mizokami Y, Osada T, Baba T, Yoshiyama M, Nishiyama J, Matsumae M (2011) Impact of the combination of 5-aminolevulinic acid-induced fluorescence with intraoperative magnetic resonance imaging-guided surgery for glioma. *World Neurosurg* 76:120–127. <https://doi.org/10.1016/j.wneu.2011.02.005>
34. Huang RY, Rahman R, Ballman KV, Felten SJ, Anderson SK, Ellingson BM, Nayak L, Lee EQ, Abrey LE, Galanis E, Reardon DA, Pope WB, Cloughesy TF, Wen PY (2016) The impact of T2/FLAIR evaluation per RANO Criteria on response assessment of recurrent glioblastoma patients treated with bevacizumab. *Clin Cancer Res* 22:575–581. <https://doi.org/10.1158/1078-0432.CCR-14-3040>
35. Choi Y, Ahn K-J, Nam Y, Jang J, Shin N-Y, Choi HS, Jung S-L, Kim B-s (2019) Analysis of heterogeneity of peritumoral T2 hyperintensity in patients with pretreatment glioblastoma: Prognostic value of MRI-based radiomics. *Eur J Radiol* 120:108642. <https://doi.org/10.1016/j.ejrad.2019.108642>
36. Hochberg FH, Pruitt A (1980) Assumptions in the radiotherapy of glioblastoma. *Neurology* 30:907–911. <https://doi.org/10.1212/wnl.30.9.907>
37. Grossman R, Shimony N, Shir D, Gonen T, Sitt R, Kimchi TJ, Harosh CB, Ram Z (2017) Dynamics of FLAIR volume changes in glioblastoma and prediction of survival. *Ann Surg Oncol* 24:794–800. <https://doi.org/10.1245/s10434-016-5635-z>

Publisher's note Springer Nature remains neutral with regard to jurisdictional claims in published maps and institutional affiliations.

Springer Nature or its licensor (e.g. a society or other partner) holds exclusive rights to this article under a publishing agreement with the author(s) or other rightsholder(s); author self-archiving of the accepted manuscript version of this article is solely governed by the terms of such publishing agreement and applicable law.